

**A major purpose of the Technical Information Center is to provide the broadest dissemination possible of information contained in DOE's Research and Development Reports to business, industry, the academic community, and federal, state and local governments.**

**Although a small portion of this report is not reproducible, it is being made available to expedite the availability of information on the research discussed herein.**

**1**

Los Alamos National Laboratory is operated by the University of California for the United States Department of Energy under contract W-7405-ENG-36

TITLE THE INFLUENCE OF ADSORBED Bi ON THE CHEMISORPTION PROPERTIES OF  
PT (111): H<sub>2</sub>, CO, and O<sub>2</sub>

AUTHORS: Mark T. Paffett, E-11  
Charles T. Campbell, CHM-2  
Thomas N. Taylor, CHM-2

REPRODUCTION OF THIS REPORT HAS BEEN REPRODUCED FROM THE BEST AVAILABLE COPY TO PERMIT THE BROADEST AVAILABILITY.

SUBMITTED TO The Journal of Vacuum Science and Technology  
American Vacuum Society, Reno, NM, December 4-7, 1984

DISCLAIMER

This report was prepared as an account of work sponsored by an agency of the United States Government. Neither the United States Government nor any agency thereof, nor any of their employees, makes any warranty, express or implied, or assumes any legal liability or responsibility for the accuracy, completeness, or usefulness of any information, apparatus, product, or process disclosed, or represents that its use would not infringe privately owned rights. Reference herein to any specific commercial product, process, or service by trade name, trademark, manufacturer, or otherwise does not necessarily constitute or imply its endorsement, recommendation, or favoring by the United States Government or any agency thereof. The views and opinions of authors expressed herein do not necessarily state or reflect those of the United States Government or any agency thereof.

By acceptance of this article the publisher recognizes that the U.S. Government retains a nonexclusive, royalty-free license to publish or reproduce the published form of this contribution or to allow others to do so for U.S. Government purposes.

The Los Alamos National Laboratory requests that the publisher identify this article as work performed under the auspices of the U.S. Department of Energy.

MASTER

Los Alamos Los Alamos National Laboratory  
Los Alamos, New Mexico 87545

THE INFLUENCE OF ADSORBED BI ON THE CHEMISORPTION PROPERTIES OF Pt(111):  
H<sub>2</sub>, CO, and O<sub>2</sub>

M. I. Paffett, C. T. Campbell, and T. M. Taylor  
Los Alamos National Laboratory  
Los Alamos, NM 87545

## ABSTRACT

The growth modes and interactions of vapor-deposited Bi on a clean Pt(111) surface and its effects on the chemisorption of  $H_2$ , CO, and  $O_2$  have been monitored by Auger electron spectroscopy (AES), low-energy electron diffraction (LEED), and thermal desorption mass spectroscopy (TDMS). For submonolayer Bi coverages, LEED patterns were observed to progress with increasing coverage through  $p(2 \times 2)$ ,  $(\sqrt{3} \times \sqrt{3})R30^\circ$ ,  $p(3 \times 3)$ , and  $p(4 \times 4)$  structures. The Bi TDMS and AES data are consistent with absolute coverages of 0.25, 0.33, 0.44, and 0.56, respectively. For submonolayer coverages of this  $s^2p^n$ -type metal, Bi adatoms are strongly repulsive and maximize their spacing subject to the constraints of the Pt(111) sites. This is to be contrasted with  $d^n s^m$ -type metals such as Ag, Cu, and Au on Pt(111), which show attractive interactions and coalesce into 2d islands. In chemisorption of small molecules on Pt(111), each Bi adatom blocks about two Pt surface atoms. An ensemble of two adjacent Pt sites is required for both dissociative  $H_2$  and molecular  $O_2$  adsorption vs one site for CO adsorption; therefore, uptake of the former adsorbates is much more severely attenuated as  $\theta_{Bi}$  increases.

## I. INTRODUCTION

There has been considerable interest in modifying the chemical reactivity of transition metal surfaces by deliberate addition of secondary metal components. A major focus of such surface science studies has been on understanding in molecular detail how the constituents of these multicomponent interfaces influence heterogeneous reactions.<sup>1,2</sup>

The present work centers on the influence that vapor-deposited Bi has on the chemical reactivity of the Pt(111) surface. In particular, the influence of adlayer growth mode on adsorption of small gaseous adsorbates (e.g. H<sub>2</sub>, CO, O<sub>2</sub>) will be addressed. The ensemble, or surface site size, requirement for adsorption will be probed for each of these molecules. Very specific contrasts will be made with previous work<sup>3-5</sup> on the influence that Group IB adatoms (Cu, Ag, Au) have on the surface chemistry of Pt(111). Qualitative interpretations concerning the growth mode characteristics displayed by these different metal adlayers (Group VB vs IB) will be favorably compared with the ideas of Bauer and Kolaczkiewicz<sup>6</sup>, who predict that the Group IB adatoms should grow in 2d islands while Bi should spread uniformly across the surface.

## II. EXPERIMENTAL

Preparation and cleaning of the Pt(111) single crystal sample is described in Ref. 3a. Surface cleanliness was ascertained by Auger electron spectroscopy (AES), low energy electron diffraction (LEED), and the size, shape, and reproducibility of O<sub>2</sub>, CO, and H<sub>2</sub> thermal desorption mass spectra (TDS). Further experimental details are listed in a related paper.<sup>3a</sup> Bismuth was vapor-deposited in the following manner. A

hemispherical reservoir for holding the Bi(5N purity) was pressed into a 0.004 in. Ta foil, which was resistively heated with 0.010 in. Ta wires spot-welded to the back. Doser temperature was monitored with a chromel-alumel thermocouple also spot-welded to the back. The Pt substrate was positioned vertically ~4 cm above the Bi reservoir, and the rest of the dosing configuration has been previously described.<sup>3a</sup> The doser was typically operated at a constant thermocouple reading of 17.75 mV (726 K), and the dose rate was measured by AES to be  $0.089 \pm 0.002$  ml min<sup>-1</sup>. (One monolayer = 1 ml = 1 Bi atom/Pt surface atom =  $1.505 \times 10^{15}$  atoms/cm<sup>2</sup> corresponds to  $\theta = 1.0$ ). The Bi/Pt(111) interfaces were grown at a substrate temperature of ~540 K followed by a 30 s anneal at ~650 K and then cooled to various temperatures for experimental characterization.

### III. RESULTS

#### A. Summary of Bi/Pt(111) Growth Modes, from Ref. 7

At submonolayer coverages, Bi adatoms form a series of ordered overlayer structures on Pt(111) as summarized in Fig. 1. The experimental evidence supporting these structural models follows from LEED, AES, and TDMS measurements described briefly here and in further detail elsewhere, where growth modes at other substrate temperatures are discussed as well.<sup>7</sup>

In the submonolayer region, LEED patterns of the Bi/Pt(111) interface were observed to progress with increasing coverage through  $p(2 \times 2)$ ,  $(\sqrt{3} \times \sqrt{3})R30^\circ$ ,  $p(3 \times 3)$ , and  $p(4 \times 4)$  structures. The structural models for these patterns, shown in Fig. 1 and consistent with TDMS and AES data,<sup>7</sup> give absolute Bi coverages ( $\theta_{Bi}$ ) of 0.25, 0.33, 0.44, and 0.56, respectively. It is apparent that Bi adatoms have significant lateral repulsions and maximize their nearest neighbor distances, resulting in hexagonal overlayers

at all these coverages. Intermediate coverages gave more complex LEED patterns, which support this model as well.<sup>7</sup> The minimum interatomic Bi-Bi distance decreases from 5.54 Å in the p(2x2) structure ( $\theta_{\text{Bi}} = 0.25$ ), to 4.80 Å in the ( $\sqrt{3} \times \sqrt{3}$ )R30° structure ( $\theta_{\text{Bi}} = 0.33$ ), to 4.16 Å in the p(3x3) structure ( $\theta_{\text{Bi}} = 0.44$ ), and finally to 3.69 Å in the p(4x4) structure ( $\theta_{\text{Bi}} = 0.56$ ). Note that the saturation p(4x4)-Bi structure has exactly the same Bi-Bi spacing as the metallic diameter of Bi (3.69 Å, as defined by Zachariasen.<sup>8</sup>) With Bi exposures greater than that necessary to achieve this saturated overlayer at  $\theta_{\text{Bi}} = 0.56$ , ordered multilayer Bi-Pt alloys are formed as discussed in Ref. 7. Bi always seems to occupy the topmost layer in these alloys, as they are inert to CO, H<sub>2</sub>, or O<sub>2</sub> chemisorption (see below, for  $\theta_{\text{Bi}} > 0.56$ ).

The Bi TDMS (m/e = 209) from surfaces with  $\theta_{\text{Bi}} < 0.56$  display a single desorption state with a peak temperature progressively decreasing from 1220 K to 1070 K as  $\theta_{\text{Bi}}$  increases.<sup>7</sup> This indicates a large decrease in the heat of adsorption ( $\sim 80 \rightarrow \sim 40$  kcal/mole), consistent with the strong lateral repulsion between Bi adatoms mentioned above. At  $\theta_{\text{Bi}} > 0.56$ , a second, lower temperature, desorption state appears with a peak temperature of  $\sim 750$  K.<sup>7</sup> This second state desorbs with zero order kinetics and an activation energy of  $53 \pm 0.5$  kcal mole<sup>-1</sup>, a value slightly higher than the sublimation energy of pure Bi, 49.5 kcal mole<sup>-1</sup>.<sup>9</sup> This second desorption state represents Bi desorption from an ordered (as evidenced by LEED) multilayer PtBi alloy surface of nominal composition Pt<sub>1.0</sub>Bi<sub>0.86</sub> (determined from AES).<sup>7</sup>

## B. Chemisorption of CO, H<sub>2</sub>, and O<sub>2</sub> at Bi/Pt(111)

The ordered Bi overlayers have a very profound influence on the chemical reactivity of the Pt(111) substrate with respect to the adsorption of CO, H<sub>2</sub>, and O<sub>2</sub>. In Fig. 2 a series of CO-TDMS traces for a saturation dose (5L) of CO at 275 K are shown for desorption from the Pt(111) surface with various Bi pre-coverages. The Pt crystal was dosed with Bi on the front and back surfaces as described previously. The TDMS traces shown in Fig. 2 have been corrected for background CO adsorption occurring at the unmasked crystal edge. The clean surface results agree with previous measurements for Pt(111).<sup>10</sup> CO will not adsorb on Bi above 100 K.<sup>11</sup>

It is readily apparent that the uptake of CO at Bi/Pt(111) is effectively attenuated upon completion of the close packed p(4x4) surface ( $\theta = 0.56$ ). There is no evidence for CO dissociation induced by Bi. Integration of the TDMS traces after background correction results in the plot of relative adsorbate coverage (CO) versus  $\theta_{Bi}$ , shown in Fig. 3. The straight line drawn in Fig. 3 represents a simple linear site blocking model for adsorption, assuming that at  $\theta_{Bi} = 0.56$ , complete filling in the Bi overlayer occurs. The CO coverage falls noticeably below that predicted by this model, although reasonably close to the dashed line in Fig. 3 which represents simple site blocking of two Pt atoms by each Bi adatom.

A similar series of experiments was conducted on the Bi/Pt(111) interface with H<sub>2</sub> as the probe molecule. It is well known<sup>12</sup> that H<sub>2</sub> dissociatively adsorbs onto Pt(111) with a saturation surface density at 150 K estimated to be  $1.20 \times 10^{15}$  atom cm<sup>-2</sup> ( $\theta_H = 0.8$ ). TDMS of hydrogen from clean Pt(111) demonstrates two states,  $\beta_1$  at ~250 K and  $\beta_2$  at 310 K.<sup>3a,12</sup> H<sub>2</sub> will not adsorb on Bi above 120 K.<sup>11</sup> Although not shown, the H<sub>2</sub> TDMS lineshapes after saturation (160 L) H<sub>2</sub> exposure to the Bi/Pt(111) interface at 150 K

looked very similar to those obtained at the Cu/Pt(111) interface<sup>3a</sup> for a given attainable hydrogen coverage (not for a given metal adlayer coverage). The  $\beta_1$  state of hydrogen was attenuated first at very low coverages of Bi ( $\theta_{Bi} < 0.05$ ). The more predominant  $\beta_2$  state was relatively unchanged in peak temperature as  $\theta_{Bi}$  increased, but it lost intensity rapidly. Upon integration and background subtraction as for Cu, the relative saturation  $H_2$  capacity of Pt(111) is shown in Fig. 3 as a function of Bi coverage. Clearly, the amount of hydrogen that can be adsorbed is much more strongly attenuated than in the CO case and displays a very nonlinear dependence on  $\theta_{Bi}$ . The curve in Fig. 3 represents the following mathematical expression:

$$\theta_H / \theta_H^0 = (1 - n\theta)^2 \quad (1)$$

where  $n = 2.2$ . The good fit of the data to this curve indicates that dissociative hydrogen adsorption requires two adjacent Pt sites, and that each Bi atom masks 2.2 Pt surface atoms. The saturation coverage on clean Pt(111),  $\theta_H = 0.8$ , tells us that 1.25 Pt surface atoms are required for each hydrogen adatom site. Note that in the model represented by Eq. (1), hydrogen adatoms are not allowed to migrate around on the surface during adsorption and pack all available sites, otherwise the quadratic dependence would disappear.

Another series of experiments were run in a manner similar to those described above, but for saturation  $O_2$  adsorption (5L) at 100 K. These data are presented and discussed in detail elsewhere<sup>7</sup> and summarized in Fig. 4. The total amount of adsorbed  $O_2$  decreases very rapidly with  $\theta_{Bi}$  and can be reasonably fit by Eq. (1) with  $n = 1.8$ . Since  $O_2$  adsorption is almost entirely molecular as a peroxo species at 110 K,<sup>13</sup> this indicates that two

adjacent Pt sites are required for molecular  $O_2$  adsorption, and that each Bi atom blocks 1.8 Pt surface atoms. The saturation coverage of  $O_{2,a}$  on Pt(111),  $\theta_{O_2} = 0.40^{13}$ , tells us that 2.5 Pt surface atoms are required for each site pair. The increase with  $\theta_{Bi}$  in the relative amount of  $O_2$  dissociating as compared to desorbing molecularly during TDMS (Fig. 4) indicates that the activation energy for dissociation of molecularly adsorbed  $O_2$  decreases significantly with Bi coverage.<sup>7</sup> The molecular desorption peak temperature, however, does not change with  $\theta_{Bi}$ .

#### IV. DISCUSSION

It is evident from the growth mode of Bi on Pt(111) that repulsive interactions between Bi adatoms play a large role in determining overlayer structures. This is to be contrasted with the cases of Cu, Ag, and Au overlayers on Pt(111), which all show dominant attractive lateral interactions leading to  $p(1 \times 1)$  island growth.<sup>3-5</sup>

Such a contrast is exactly that predicted in a recent review by Bauer and Kolaczkiewicz.<sup>6</sup> Based upon experimental results from a variety of submonolayer metal films on "smooth" (i.e., (110) in BCC) transition metal surfaces, these authors classified adsorbate metals according to the nature of their lateral interactions in the adsorbed layers. Strongly repulsive interactions are observed for alkali and alkali earth metals, since these bond ionically and therefore experience significant dipole-dipole repulsion in the adlayer. Weakly repulsive interactions are observed for metals such as Bi, Sb, Pb, Tl, Te, and Hg, of the  $s^2 p^n$ -type electronic configuration. Here the electronegativity difference with the substrate is small, and only weak dipole-dipole repulsions result. The heat of sublimation of these metals is small ( $\sim 50$  kcal mole<sup>-1</sup> for Bi), indicating only a weak binding

energy in the solid. These are strongly bound to the substrate at low coverage [ $180 \text{ kcal mole}^{-1}$  for Bi/Pt(111)<sup>7</sup>], so that no electrons are available for lateral bonding. Instead, the lateral interaction is repulsive, presumably due to the small dipole repulsions and also indirect repulsions via the substrate electrons. Attractive interactions are seen for adsorbates such as Cu, Ag, Au, Ni, and Pd, which have the  $d^n s^n$ -type configuration. Here again, small electronegativity differences give rise to weak dipole repulsions, which in this case, however, are overcome by the availability of electrons for forming lateral attractive bonds. For these metals, the heat of sublimation is much larger ( $80.5 \text{ kcal mole}^{-1}$  for Cu),<sup>9</sup> indicating stronger bonding in the solid.

As pointed out by Bauer and Kolaczkiewicz,<sup>6</sup> these classes of lateral interactions are manifested clearly in the growth modes and LEED patterns for the overlayers on smooth surfaces. Attractive interactions lead to 2d condensation into islands of high local coverage already from very low average coverage. Repulsive interactions lead to structures below saturation in which the adatoms maximize their lateral distances, subject to the constraints induced by the potential modulation of the substrate. These constraints are more clearly seen for the case of weak than for strong repulsion. We see that these different growth modes give rise to striking differences in the effects of the foreign metal adatoms on the chemisorption properties and reactivity of the resulting surface. Metals with attractive interactions that form 2d islands produce composite surfaces, which have chemisorption properties only slightly different than a linear combination of the properties of the separate metals (scaled by  $\theta$ ). Thus, for Cu and Ag (which do not adsorb CO or H<sub>2</sub> at the temperatures used), on Pt(111)<sup>3a</sup> or Rh(100)<sup>14</sup>, the CO and hydrogen

adsorption capacity decreases linearly with coverage to almost zero at  $\theta = 1.0$ . Metals with strong repulsive interactions due to large charge transfer can have a strong electronic influence on the chemisorption properties of the substrate. This is the case with K on Pt(111) for example.<sup>15</sup> Metals with weak repulsive interactions and little charge transfer to the substrate will not have such strong electronic effects, but since they spread fairly evenly over the surface, they will give rise to what are known as "ensemble" effects upon chemisorption. "Ensemble" refers to the number and geometry of adjacent metal atoms or sites required for chemisorption or a surface reaction. Dissociative chemisorption of  $H_2$ , for example, is generally thought to require an ensemble of two adjacent sites to accommodate the two hydrogen adatoms produced.

For the case of Bi on Pt(111), ensemble effects are clearly at play in the results for  $H_2$  and  $O_2$  adsorption in Figs. 3 and 4. The data are reasonably fit by models [Eq. (1)] in which an ensemble of two adjacent sites are required for both dissociative  $H_2$  adsorption and molecular (peroxo-)  $O_2$  adsorption, whereby each Bi adatom, due to its size, blocks 2.2-1.8 Pt surface atoms. Note that saturation coverage ( $\theta_{R1} = 0.56$ ) corresponds to one Bi atom for every  $1/0.56 = 1.78$  Pt(111) surface atoms. The requirement of two adjacent sites for molecular  $O_2$  adsorption is consistent with the fact that  $O_2$  is thought to lie parallel to the Pt(111) surface.<sup>13b</sup> The CO data of Fig. 3 can be fit by a model in which only a single site is required by molecular CO adsorption, where each Bi adatom blocks 2.0 Pt surface atoms. Only a single site is required for  $CO_a$ , since its bond is perpendicular to Pt(111).<sup>16</sup> One can, of course, derive more microscopic detail concerning the ensemble requirement in adsorption through careful inspection of the structural models in Fig. 1.

The major point we would like to make here concerns the choice of adsorbate metal when attempting to probe ensemble effects in chemisorption and catalysis. Most work in the past has focussed on adsorbates such as Ag, Cu, or Au, which are particularly poor choices since lateral attraction leads to 2d island condensation. Metals such as Bi, which have the  $s^2p^n$ -type configuration, are much better prospects, since these spread uniformly across the surface and yet have similar electronegativities, so that the electronic influence on the substrate is minimal. These metals are also often very inert in chemisorption, as is Bi.<sup>14</sup>

Note the significant narrowing of the CO-TDMS peaks to lower temperature in Fig. 2 when  $\theta_{Bi}$  exceeds 0.15. As Bi is slightly more electropositive than Pt, any charge transfer or ligand effect would be expected to give the opposite result. (For example, K increases the desorption energy for CO on Pt(111).<sup>15</sup> Interestingly, the lineshape and position for CO desorption when  $\theta_{Bi} > 0.15$  in Fig. 2 match almost exactly those for CO desorption from Pt(111) when only desorption from the bridge-bonded CO is monitored. (The deconvolution of the spectrum in Fig. 2 for clean Pt(111) into components for linear and bridge-bonded CO was cleverly mastered by Norton, et al.,<sup>16a</sup> using dynamic work function measurements). This may indicate that Bi adsorption rapidly masks the sites necessary for the more strongly bonded linear CO on Pt(111), and only bridge-bonded linear CO is populated for  $\theta_{Bi} > 0.2$ . EELS measurements as in Ref. 16b would be useful to test this hypothesis.

A comparison of the relative effects of underpotentially deposited Bi, Ag, and Cu upon electrochemical hydrogen adsorption from acidic solution onto polycrystalline Pt electrodes has been presented.<sup>17</sup> In these cases, the amount of adsorbed hydrogen is linearly attenuated with metal coverage. The

two-site ensemble effect such as demonstrated in Fig. 3 for Bi does not appear, presumably since  $H_2$  dissociation is not required in the electrochemical process. The size difference between Bi and Cu or Ag, is however, also seen in the electrochemical measurements, with only about half the Bi coverage required to achieve the same amount of hydrogen attenuation as of Cu or Ag.

#### ACKNOWLEDGMENTS

Support by the Department of Energy, through the Morgantown Energy Technology Center, Phosphoric Acid Fuel Cell Program, is gratefully acknowledged by MTP. Partial support by the Department of Energy, Division of Basic Energy Sciences, is gratefully acknowledged by TNT and CTC. Helpful discussions with Roy Feber are a pleasure to acknowledge.

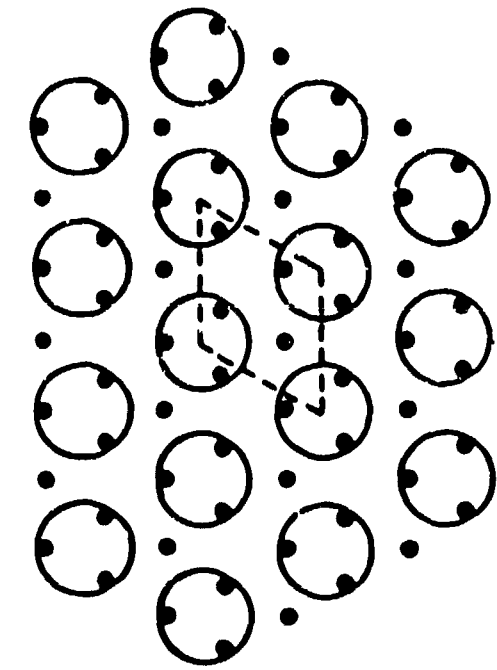
## References

1. G. A. Somorjai, Chemistry in Two Dimensions: Surfaces, Cornell University Press, 1981.
2. D. M. Kolb, Advances in Electrochemistry and Electrochemical Engineering, H. Gerischer, Ed., J. Wiley, 1978.
3. a) M. T. Paffett, C. T. Campbell, T. N. Taylor, and S. Srinivasan, submitted to Surface Sci.  
b) K. C. Yeates and G. A. Somorjai, Surface Sci. 134, 729 (1983).
4. a) M. T. Paffett, C. T. Campbell, and T. N. Taylor, to be submitted to Surface Sci.  
b) P. W. Davies, M. A. Quinlan, and G. A. Somorjai, Surface Sci. 121, 290 (1982).
5. J. W. Sachtler and G. A. Somorjai, J. Catal. 81, 77 (1983).
6. E. Bauer and J. Kolaczkiwicz, Proc. IX Intern. Vacuum Con. and V. Intern. Con. Solid Surfaces, Madrid (1983) 363.
7. M. T. Paffett, C. T. Campbell, and T. N. Taylor, manuscript in preparation.
8. W. H. Zachariassen, J. Inorg. Nucl. Chem. 35, 3487 (1973), Eq. (1), where we used the bulk density of Bi ( $9.8 \text{ g cm}^{-3}$ ) to obtain its atomic volume.
9. R. Holtgren, P. D. Desai, D. T. Hawkins, M. Gleiser, K. K. Kelley, and D. D. Wagman, Selected Values of the Thermodynamic Properties of the Elements, American Society for Metals, 1973.
10. C. T. Campbell, G. Ertl, H. Kuipers, and J. Segner, Surface Sci. 107, 207 (1981).
11. T. N. Taylor, C. T. Campbell, J. W. Rogers, Jr., W. P. Ellis, and J. M. White, *ibid.* 134, 529 (1983).
12. K. Christman, G. Ertl, and T. Pignat, *ibid.* 54 365 (1976).
13. a) J. L. Gland, *ibid.* 93, 487 (1980).  
b) J. L. Gland, B. A. Sexton, and G. B. Fisher, *ibid.* 95, 587 (1980).
14. H. C. Peebles, D. D. Beck, J. M. White, and C. T. Campbell, *ibid.* in press.
15. H. P. Bonzel, J. Vac. Sci. Technol. A2, 866 and ref. therein (1984).
16. a) P. R. Norton, J. W. Goodale and E. B. Selkirk, Surface Sci. 83, 189 (1979).  
b) H. Steininger, S. Lehwald, and H. Ibach, *ibid.* 123, 264 (1982).
17. M. Furuya and S. Motoo, J. Electroanal. Chem. 157, 139 (1983).

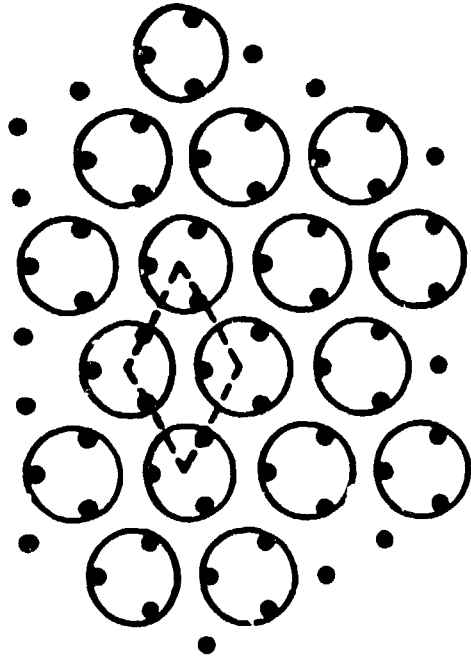
## Figure Captions

- Fig. 1 Structural models of submonolayer Bi on Pt(111) determined from LEED patterns and AES.<sup>7</sup> Platinum atoms represented by (●) and bismuth atoms by large spheres. Unit cells are shown by the dashed lines. Surface preparation described in text.
- Fig. 2 CO thermal desorption spectra resulting from a saturation exposure (5L) of CO for various Bi pre-coverages on Pt(111). Sample temperature was 275 K for CO dose. The heating rate (β) is 13.1 Ks<sup>-1</sup>.
- Fig. 3 Saturation adsorption capacity of Pt(111) for CO and H<sub>2</sub> adsorption as a function of Bi pre-coverage. The relative adsorbate coverage is determined from the areas under TDMS traces such as Fig. 2 for CO. (○) 5L-CO dose at 275 K. (●) 200L-H<sub>2</sub> dose at 150 K. These exposures were sufficient for saturation at all Bi coverages. Solid and dashed lines described in text.
- Fig. 4 Summary of TDMS results after a saturation O<sub>2</sub> dose (5L) to Pt(111) at 110 K containing various pre-coverages of Bi. (●) Total O<sub>2</sub> adsorption capacity as measured by the sum of areas under the O<sub>2</sub> desorption peaks for both molecularly (164 K) and atomically (-700 K) adsorbed oxygen. (○) Ratio of O<sub>2</sub> desorbing in the atomic peak to that desorbing in the molecular peak.

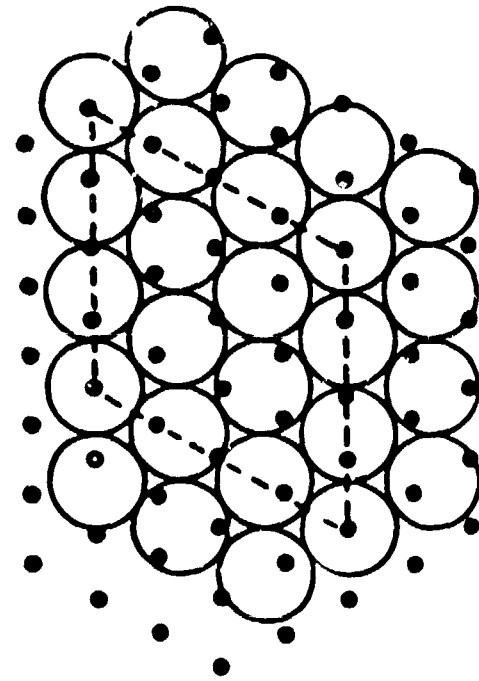
Bi/Pt(111)



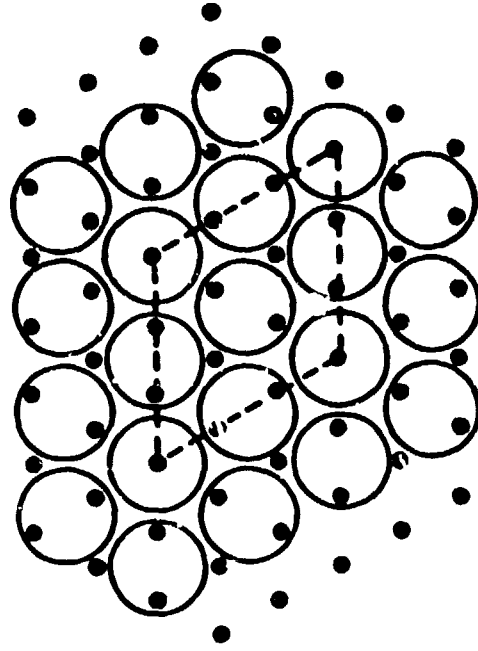
$p(2 \times 2), \theta_{Bi} = 0.25$



$(\sqrt{3} \times \sqrt{3})R30^\circ, \theta_{Bi} = 0.33$



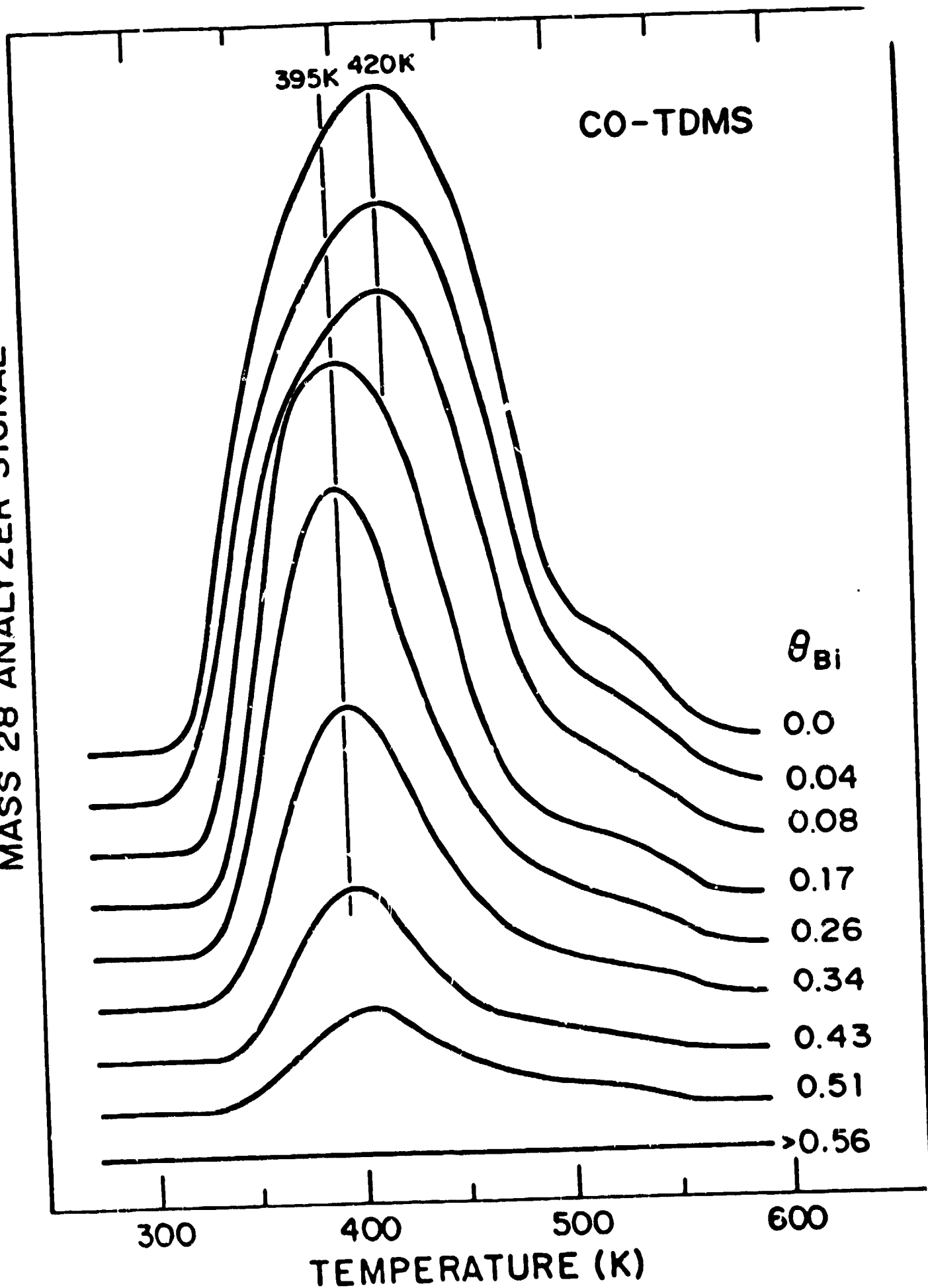
$p(4 \times 4), \theta_{Bi} = 0.56$



$p(3 \times 3), \theta_{Bi} = 0.44$

Fig 1

MASS 28 ANALYZER SIGNAL



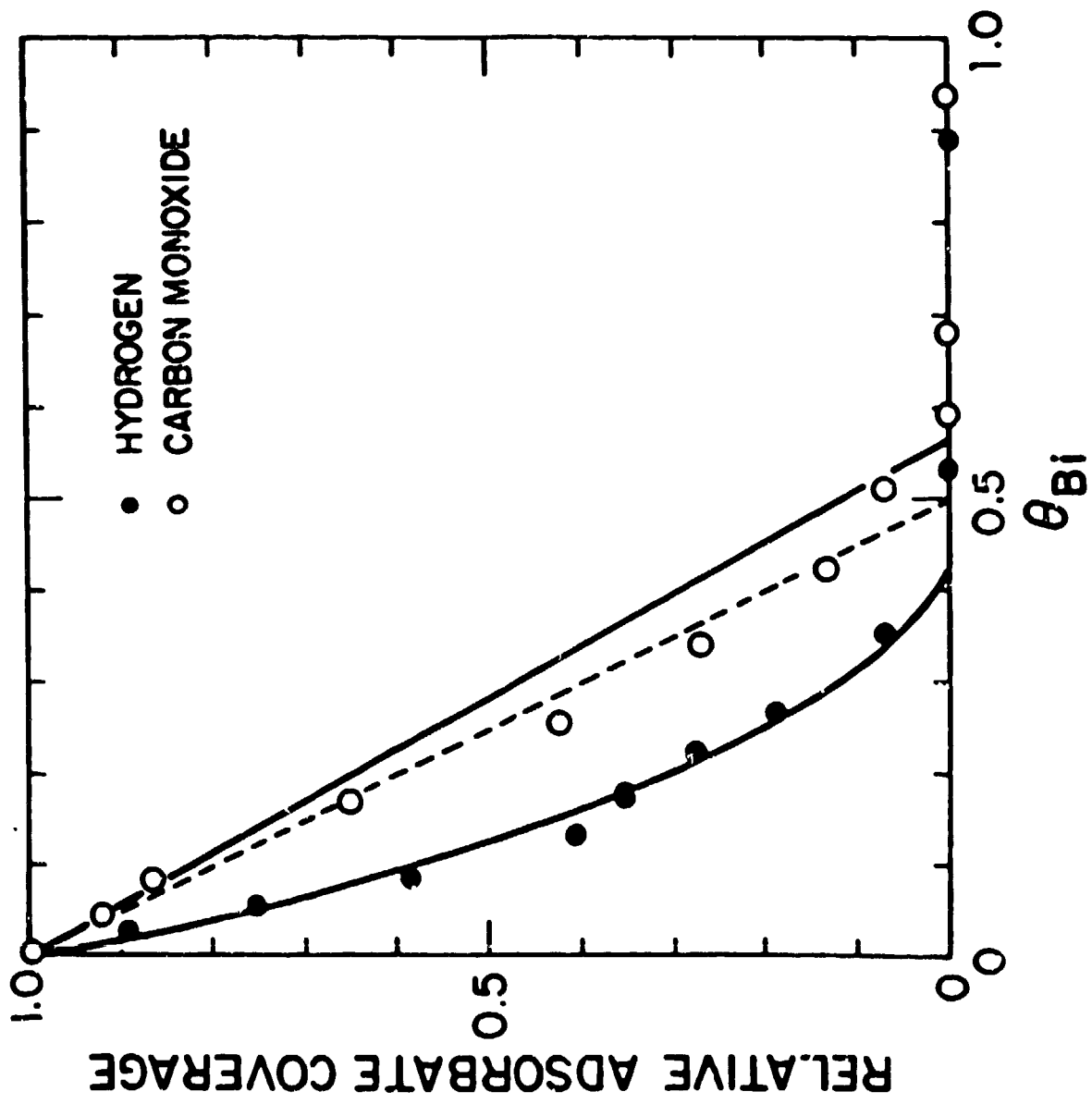


Fig. 3

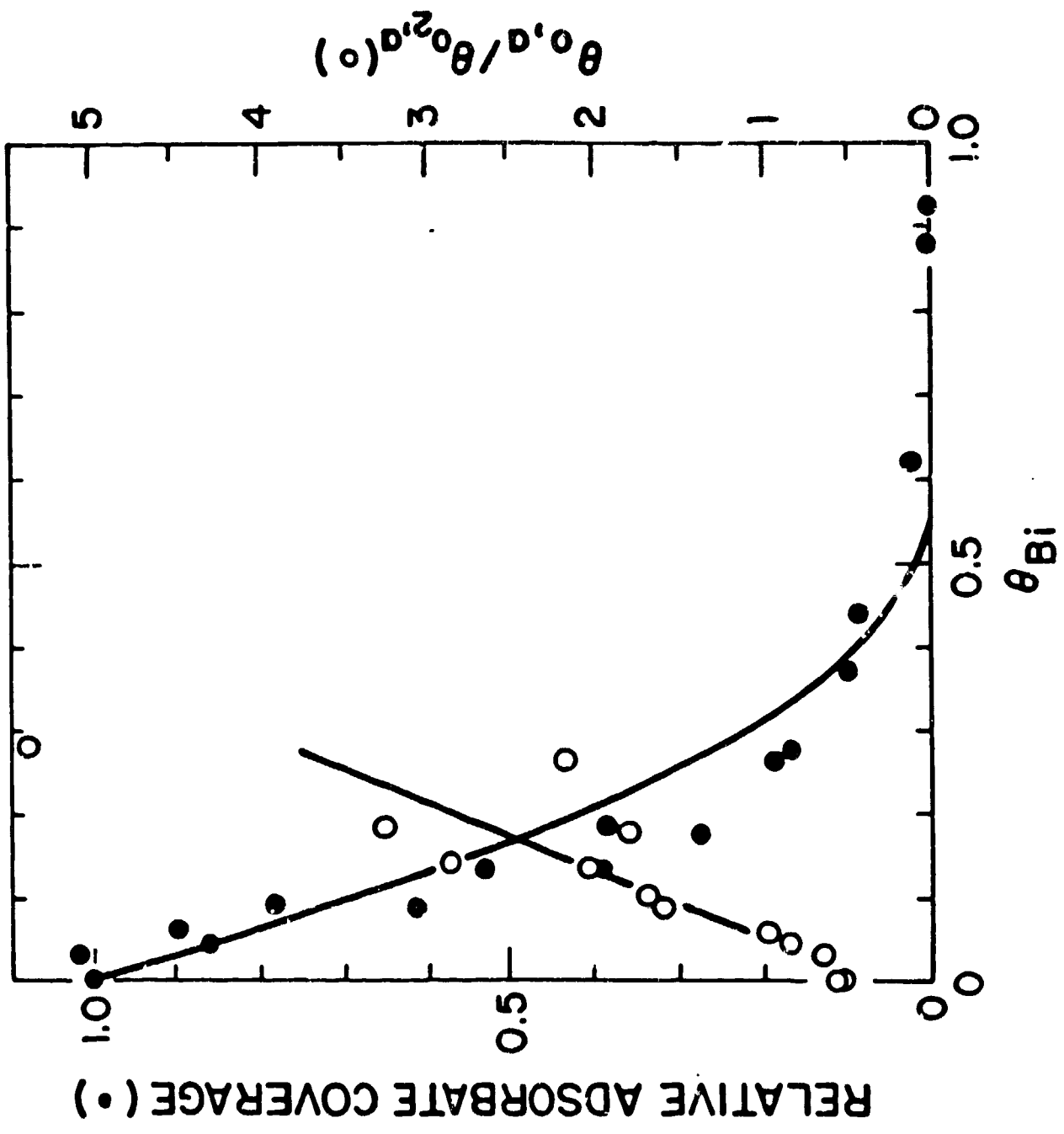


Fig. 4